Mean velocity scaling of high-speed turbulent flows under non-adiabatic wall conditions

Khaled Younes*
Department of Mechanical Engineering, Stanford University, Stanford, CA 94305, USA

Jean-Pierre Hickey†
Department of Mechanical and Mechatronics Engineering, University of Waterloo, Waterloo, ON N2L 3G1, Canada

The problem of scaling the near-wall mean velocity profiles of turbulent flows and collapsing them with the law of the wall has been traditionally studied using the conservation of momentum, by employing various levels of assumptions. In the van Driest transformation ("Turbulent Boundary Layer in Compressible Fluids," ***Journal of the Aeronautical Sciences*****, Vol. 18, No. 3, 1951, pp. 145–216), the viscous stress was neglected, whereas in the Trettel and Larsson transformation ("Mean Velocity Scaling for Compressible Wall Turbulence with Heat Transfer,"** ***Physics of Fluids*****, Vol. 28, No. 2, 2016, Paper 026102), the Reynolds stress was assumed to cancel out. Recent work by Griffin, Fu, and Moin ("Velocity Transformation for Compressible Wall-Bounded Turbulent Flows with and Without Heat Transfer,"** ***Proceedings of the National Academy of Sciences of the United States of America*****, Vol. 118, No. 34, 2021, Paper e2111144118) used a quasi-equilibrium assumption between turbulence production and dissipation in the log layer and demonstrated success for a wide variety of canonical flows. However, the extent of quasi-equilibrium is not verified, particularly for non-canonical flows. In this work, an alternate transformation is developed using the semi-local gradient of the van Driest transformed velocity, which is principally tied to the dynamics of vorticity transport in the boundary layer. In addition, a modified stress balance is utilized to directly account and scale the buffer region. The transformation was benchmarked using a similar dataset as in Griffin** ***et al*****, and similar performance was obtained. Moreover, at supercritical pressures, the present transformation is found to produce significantly better collapse than existing works.**

Nomenclature

C = law of the wall additive constant, $C = 5.2$

h = channel half-height, m

*PhD Candidate, Department of Mechanical Engineering; kyounes@stanford.edu (Corresponding Author).
†Assistant Professor, Department of Mechanical and Mechatronics Engineering; jean-pierre.hickey@uwaterloo.ca.

P	=	turbulence kinetic energy production, Pa/s
$P^{\ddagger}$	=	normalized turbulence kinetic energy production, $P^{\ddagger} = -\bar{\rho}^{+}\overline{u'v'}^{+}\dfrac{d\bar{u}^{+}}{dy^{*}}$, Pa/s
S	=	pre-multiplied mean shear, Pa
T	=	temperature, K
u	=	streamwise velocity, m/s
u_τ	=	friction velocity, $u_\tau = \sqrt{\tau_w/\rho_w}$, m/s
u_τ^*	=	semi-local friction velocity, $u_\tau^* = u_\tau\sqrt{\rho_w/\bar{\rho}}$, m/s
v	=	wall-normal velocity, m/s
y	=	wall-normal distance, m
y_τ	=	viscous length scale, $y_\tau = \mu_w/(\rho_w u_\tau)$, m
y_τ^*	=	semi-local length scale, $y_\tau^* = \bar{\mu}/(\bar{\rho}u_\tau^*)$, m
ϵ	=	viscous dissipation, Pa/s
$\epsilon^{\ddagger}$	=	normalized viscous dissipation, $\epsilon^{\ddagger} = \epsilon^{+}/\bar{\mu}^{+}$, Pa/s
κ	=	von Kármán's constant, $\kappa = 0.41$
μ	=	dynamic viscosity, kg/(m·s)
ω_z	=	spanwise vorticity, Hz
ϕ	=	mapping function, Pa
ρ	=	density, kg/m^3
Re_τ	=	friction Reynolds number
Re_b	=	bulk Reynolds number
τ	=	shear stress, Pa

Subscripts

b	=	variable associated with the buffer sublayer
eq	=	variable obtained via the quasi-equilibrium assumption
GFM	=	variable associated with the Griffin, Fu, and Moin transformation
R	=	Reynolds stress variable
t	=	variable obtained via a total stress balance
TL	=	variable associated with the Trettel and Larsson transformation
w	=	wall variable
v	=	viscous stress variable
vD	=	variable associated with the van Driest transformation

Superscripts

$\bar{()}$ = Reynolds-averaged variable

$()^+$ = variable normalized by wall units, $(\cdot)^+ = (\cdot)/y_\tau$

$()'$ = fluctuation around a Reynolds-averaged variable

$()^*$ = variable normalized by semi-local units, $(\cdot)^* = (\cdot)/y_\tau^*$

I. Introduction

The quest for universal laws that govern the chaotic behavior of turbulence is not new. Yet, today, and despite several decades of research, the two triumphs of turbulence theory remain arguably Kolmogorov's $4/5$-th law [1], which describes the energy cascade from large eddies into smaller ones, and von Kármán's law of the wall [2]. The latter in particular has been a staple in collapsing the near-wall velocity profiles of seemingly very different, incompressible boundary layer and channel flows into a single semi-analytical function. Accordingly, it has allowed engineers and researchers to develop wall models that capture the velocity in the near-wall region. Its mere existence and wide applicability in the case of incompressible wall-bounded flows has further motivated fluid dynamicists to seek transformations that scale any type of flow—regardless of the boundary condition, pressure gradient, surface roughness, and degree of compressibility—to match with the original law of the wall formulation [2]:

$$u^+ = \frac{1}{\kappa}\ln(y^+) + C \qquad \text{for} \qquad 30 \lesssim y^+ \lesssim 150. \tag{1}$$

Together with the viscous sublayer relation, $u^+ = y^+$ for $y^+ < 5$, Eq. (1) forms the current paradigm in wall-bounded incompressible turbulence.

In the context of compressible flows, the focus of this paper, a transformation was presented by van Driest [3], who was the first to show that a mapping from the compressible state back to the incompressible reference was indeed possible:

$$u^+_{vD} = \int_0^{u^+} \sqrt{\frac{\bar{\rho}}{\rho_w}}\, du^+. \tag{2}$$

The van Driest transformation was widely considered to be the state-of-the-art in velocity transformations. However, when research into supersonic and hypersonic flows started to emerge in the 1960's [4], its shortcomings were identified. For under those high-speed flow conditions, viscous heating at the wall causes a significant increase in wall temperature—one that cannot be withstood by common aerospace materials. As such, external wall cooling was employed for engineering applications; and it happens to be precisely under those non-adiabatic wall conditions that the van Driest transformation fails to collapse the velocity profiles with the law of the wall [4].

The mismatch spurred numerous reconciliation attempts. In early work, Danberg [4] tried to correlate the discrepancy with the freestream Mach number and heat transfer, but his findings were inconclusive. Four decades later, Brun *et al.* [5] ran large eddy simulations (LES) of compressible channel flows and applied the transformation of Cope and Hartree [6] to the resulting velocity profiles. They noted significant improvement in the collapse in the viscous sublayer, but the logarithmic region remained unreconciled. Following that, Zhang *et al.* [7] and Pei *et al.* [8] presented new scaling using an extension of Townsend's structure parameter and a concept of velocity-vorticity correlation structure, respectively. The transformed profiles displayed Mach number invariance, yet they were not independent of the wall heat transfer.

In more recent efforts, Trettel and Larsson [9] and Patel *et al.* [10] succeeded independently in deriving a transformation that collapsed the non-adiabatic, compressible velocity profiles with the incompressible law of the wall [9, 10]:

$$u^+_{TL} = \int_0^{u^+} \sqrt{\frac{\bar{\rho}}{\rho_w}} \left(1 + \frac{1}{2}\frac{1}{\bar{\rho}}\frac{d\bar{\rho}}{dy}y - \frac{1}{\bar{\mu}}\frac{d\bar{\mu}}{dy}y\right) du^+. \tag{3}$$

The Trettel and Larsson transformation proved to be robust and accurate when studying non-adiabatic channel flows [9]. When applied to high-speed boundary layer flows, though, the transformation failed in the log layer [11]. To remedy that, Wu *et al.* [12] proposed a new transformation using a modification of Prandtl's mixing layer assumption, dividing the flow into three distinct sub-regions. In addition, Volpiani *et al.* [13] built on the work of Modesti and Pirozzoli [14], who recast all the known transformations into a general set of mapping functions, and implemented a data-driven approach to match the compressible velocity profiles with the incompressible reference. Both works yielded a slight improvement in the collapse, but the mismatch was nonetheless still observed [13]. Most recently, Griffin *et al.* [15] succeeded in reconciling the mismatch by proposing a transformation that combines the near-wall asymptotic behavior of the Trettel and Larsson transformation [9] along with the assumption of quasi-equilibrium, between turbulence production and dissipation, in the log layer. However, two issues not addressed by their transformation remain: (1) the extent of the underlying assumptions used to arrive at quasi-equilibrium, and (2) the buffer layer is not explicitly accounted for.

In this work, starting from a detailed analysis of the van Driest [3], Trettel and Larsson [9], and Griffin *et al.* [15] transformations in §II, we identify why and under what conditions does each succeed and fail. Moreover, we also revisit the quasi-equilibrium assumption of Griffin *et al.* [15] in §II and derive an alternate transformation that incorporates a direct scaling for the buffer region. §III assesses the performance of the new scaling and discusses its implications. Concluding remarks are given in §IV.

II. Analysis

The main premise behind any successful mean velocity transformation is the existence of a normalized function, $\phi^\dagger = du^+/dy^\dagger$, whose dependence is only on the wall-normal coordinate. Thus, when integrated, a collapse among the velocity profiles in the near-wall region will be seen. Mathematically, this translates to:

$$u^+ = \int_0^{y^\dagger} \phi^\dagger(y^\dagger) dy^\dagger, \tag{4}$$

where traditionally the wall-normal coordinate has been either obtained by non-dimensionalizing by wall units or from semi-local arguments, i.e. $y^\dagger = y^+$ or y^*. By recasting the transformations in the form presented by Eq. (4), the failure of any given one can now be viewed as a breakdown of the invariance of $\phi^\dagger$ to the wall-normal coordinate of choice. In other words, if the mathematical mapping contained in $\phi^\dagger$, which can be physically thought of as a non-dimensionalized mean shear quantity, is found to depend on any global variable in the flow, it is expected that the said transformation will not succeed in collapsing the profiles with the incompressible law of the wall. From this lens, the three most successful transformations in the literature can be studied.

A. Previous Transforms

1. Van Driest Transformation

In the van Driest (vD) transformation [3], the wall-normal coordinate is assumed to be y^+. Then, Eq. (2) can be rewritten as:

$$u^+_{vD} = \int_0^{y^+} \sqrt{\frac{\bar{\rho}}{\rho_w}} \frac{du^+}{dy^+} dy^+, \tag{5}$$

where $\phi^+_{vD}(y^+) = du^+_{vD}/dy^+ = \sqrt{\bar{\rho}^+} du^+/dy^+$. Patel *et al.* [10] plot ϕ^+_{vD} $vs.$ y^+ for a wide variety of channel flows with different fluid behaviors; gas-like, liquid-like, and constant property flows were studied, in addition to adiabatic and non-adiabatic wall conditions. In all the cases considered, it was shown that $\phi^+_{vD} = f(y^+)$ remains invariant to the flow condition as long as the walls are adiabatic. Furthermore, when the walls are externally cooled or heated, the profiles of $\phi^+_{vD}(y^+)$ deviate from one another starting from the viscous sublayer. The precise discrepancy is thought to be dependent upon the gradient of the semi-local friction Reynolds number, dRe^*_τ/dy [10]. Collectively, the aforementioned observations explain why the vD transformation remains remarkably accurate for high-Mach number flows (with adiabatic walls) well into the supersonic and hypersonic regime [16] but fails entirely for flows with non-adiabatic wall conditions, irrespective of the freestream Mach number [10, 17].

This finding can also be tied to the mechanism of vorticity generation and transport in the boundary layer, since ϕ^+_{vD} is equivalent to the mean spanwise vorticity normalized by wall units, $\bar{\omega}^+_{z,vD}$. As Pirozzoli and Bernardini [18] find, $\bar{\omega}^+_{z,vD}$ is invariant to the flow conditions when plotted against y^+ for adiabatic walls. Given that vorticity generated at the wall is first transported by viscosity in the viscous-dominant viscous sublayer and then carried outward by turbulent transport in the buffer region [19], it is unsurprising that in the absent of strong gradients in viscosity brought about by non-adiabatic wall conditions, the vD transformation holds.

It is worth noting that an alternate derivation for the vD transformation can also be followed using the averaged form of the conservation of x-momentum: by assuming a constant stress layer in the near-wall region, neglecting the viscous contribution, and resolving the Reynolds (turbulent) stress using Prandtl's mixing length. The final result will be identical to that in Eq. (5), however, the physical mechanism for failure differs slightly. From the conservation of momentum perspective, the structure of the boundary layer changes significantly when the walls are externally cooled. In particular, it is known that the buffer layer thickens drastically with wall cooling [17]. This inherently means that the log region, where the Reynolds stress is most dominant, will be pushed farther away from the wall. Accordingly, the vD transformation, which takes no account of the contributions of the viscous and buffer sublayers, will fail immediately adjacent to the wall.

2. Trettel and Larsson Transformation

In contrast to the vD transformation, Trettel and Larsson [9] derive the wall-normal coordinate to be the semi-local y^*. In that regard, $y^\dagger = y^*$ and Eq. (3) can be reformulated using the chain rule:

$$u^+_{TL} = \int_0^{y^*} \frac{\bar{\mu}}{\mu_w} \frac{dy^*}{dy^+} \frac{du^+}{dy^*} dy^*, \tag{6}$$

where $\phi^*_{TL}(y^*) = du^+_{TL}/dy^* = \bar{\mu}^+ du^+/dy^+$. Substituting the definition of y^* and y^+ and performing the differentiation dy^*/dy^+ in Eq. (6) recovers the original form of the Trettel and Larsson (TL) transformation. The TL transformation can be obtained from a similar stress balance as in the vD transformation, but by canceling out the Reynolds stress using Morkovin's hypothesis [20] and scaling the viscous stress instead [21]. (It was shown in [22] that the vD and TL transformations can be generalized using a single variable.) The reason for the success of the TL transformation in channel flows and failure in boundary layer flows was not immediate. However, the work of Patel *et al.* [10] shed more light onto the matter, since they showed that $\phi^*_{TL}(y^*)$ is invariant to the flow condition in the entire near-wall region when plotted against y^* in channel flows, but it displays dependence on Re^*_τ in the log layer for boundary layer flows. (Patel *et al.* [10] specifically plot $(h/Re^*_\tau)(d\bar{u}_{VD}/dy)$ against the semi-local coordinate; this quantity is equivalent to ϕ^*_{TL} in the present paper.) Therefore, it is expected that the TL transformation will fail in the log region for boundary layer flows, regardless if the walls are externally cooled or not, and it will collapse the near-wall mean velocity profiles from channel flows (with or without wall cooling). The direct numerical simulations (DNS) of Wu *et al.* [12], Volpiani *et al.* [23, 24], Zhang *et al.* [11], Modesti and Pirozzoli [14, 25], Huang *et al.* [26, 27], Yao and Hussain [28], and Cogo *et al.* [29] all appear to support this hypothesis.

3. Griffin, Fu, and Moin Transformation

Griffin, Fu, and Moin (GFM) take a different approach in deriving their transformation. Namely, as opposed to seeking a single variable that provides a universal collapse when plotted against some wall-normal coordinate, they split the near-wall region into two distinct entities, the viscous sublayer and log region, and find mappings applicable to each individually. They choose y^* as the basis of their scaling, motivated by the success of the semi-local coordinate in collapsing the near-wall turbulence statistics [30]. Following that, a total stress balance is applied to yield a continuous transformation for the whole inner layer [15]. Their transformation writes:

$$u^+_{GFM} = \int_0^{y^*} S^+_t dy^*, \tag{7}$$

where

$$S^+_t = \frac{S^+_{eq}}{1 + S^+_{eq} - S^+_{TL}} \tag{8}$$

under the constant stress layer assumption ($\tau^+ \approx 1$). In Eq. (8), $S^+_{TL} = \phi^*_{TL}$ is used to scale the viscous region and $S^+_{eq} = (1/\bar{\mu}^+)(du^+/dy^*)$ is applied in the log layer. While ϕ^*_{TL} has been addressed in detail by Trettel and Larsson [9], Patel *et al.* [10], and in §II.A.2, the underlying assumptions utilized to get S^+_{eq} warrant a mention. According to Griffin *et al.* [15], S^+_{eq} nestles on three primary assumptions in the log layer: the Mach-invariance of (1) $P^\ddagger/\epsilon^+$, (2) $\epsilon^\ddagger$, and (3) τ^+_R with respect to y^*. The third assumption broadly belongs to Morkovin [20], who postulated that the Reynolds stress in the near-wall region scales with τ_w, while the first two are based on an extension of the ideas put forth by Zhang *et al.* [7] on the balance of turbulent kinetic energy (TKE) production and dissipation; Griffin *et al.* [15] generalize those ideas as a function of the semi-local coordinate, but they do not validate them separately. This is addressed next.

B. Revisiting the Quasi-Equilibrium Assumption

First, the scope of Morkovin's scaling has been investigated extensively in the past (see, e.g., [16, 27, 30, 31]). It was concluded from all the efforts that the semi-local wall-normal coordinate, y^*, better collapses the turbulence statistics, including the Reynolds stress τ^+_R, up to the buffer layer ($y^* \leq 10$). In the log region, however, Reynolds number effects do persist [10, 27, 30], and it cannot be assumed that τ^+_R is truly invariant against y^*. This can be more readily seen in the boundary layer DNS of Zhang *et al.* [11] and Cogo *et al.* [29], where a direct collapse among the profiles of τ^+_R is only present when the semi-local friction Reynolds number, Re^*_τ, is matched. As a result, this suggests that $\tau^+_R = f(y^*, Re^*_\tau)$ in the log layer, and τ^+_R cannot be used as a basis for the scaling in that region. (While the profiles of τ^+_R do not display dependence on the Mach number, the variable $\phi^\dagger$ must only be a function of the wall-normal coordinate in order to get a universal scaling.) A similar observation was made by Patel *et al.* [10] in their channel flow simulations.

Second, the definition of $\epsilon^{\ddagger}$ according to Griffin *et al.* [15] indicates that it is a normalized solenoidal dissipation, non-dimensionalized by wall units. As such, it is not clear how it varies as a function of a semi-local quantity, y^*, especially since $y^* \neq y^+$ in general; in fact, the two are related by the ratio of Re_τ / Re_τ^*, which is only unity when $\sqrt{\bar{\rho}^+}/\bar{\mu}^+ = 1$. Analogously, $P^{\ddagger}$ is a semi-local quantity, while ϵ^+ is normalized by the values at the wall. Despite that, the GFM transformation produces excellent collapse for a wide range of flows—channel, pipe, and boundary layer flows [15]. This begs the question of how it achieves so. A possible explanation is that the Re_τ^* dependence of τ_R^+ in $P^{\ddagger}$ exactly counteracts the dependence on Re_τ / Re_τ^* in $\epsilon^{\ddagger}$, which appears in the denominator of $P^{\ddagger}/\epsilon^+$. If so, then an invariant scaling using the quasi-equilibrium assumption would be plausible. In fact, it will be shown later that the balance between Re_τ^* and Re_τ / Re_τ^* need not be perfect, at least not in the log layer, as an approximate cancellation in the buffer layer is sufficient to cause an acceptable collapse in the velocity profiles. Since the transformations are written in integral form, a small deviation in the buffer layer compounds significantly in the log region, whereas a large discrepancy in the log layer does not strongly influence the scaling.

C. Proposed Transformation

To derive our transformation, we retain the idea of dividing the boundary layer into separate regions and scaling each on its own as a function of y^*. However, instead of relying on quasi-equilibrium between TKE production and dissipation in the log region as was done by Griffin *et al.* [15], we hypothesize that the following relation holds outside the viscous and buffer sublayers:

$$\phi_{vD}^* = \frac{du_{vD}^+}{dy^*} = f(y^*). \tag{9}$$

Physically, ϕ_{vD}^* represents a semi-local normalized mean spanwise vorticity, similar to how ϕ_{vD}^+ was linked to $\bar{\omega}_{z,vD}^+$. By utilizing y^* in Eq. (9), in contrast with y^+ in ϕ_{vD}^+, it is expected that property variations in the log layer will now be accounted for in the mechanism of vorticity transport. Furthermore, to directly factor for the buffer layer, we propose modifying the basis of the scaling. Starting from a stress balance in the near-wall region:

$$\tau_v^+ + \tau_R^+ = \tau^+, \tag{10}$$

and multiplying Eq. (10) by τ^+, we get:

$$\tau_v^{+2} + 2\tau_v^+\tau_R^+ + \tau_R^{+\,2} = \tau^{+2}, \tag{11}$$

where the second term on the left-hand side is active mostly in the buffer layer. A normalized form of Eq. (11) can be written as follows:

$$\left(\frac{\tau_v^+}{\phi_{TL}^*}\right)^2 + 2\frac{\tau_v^+\tau_R^+}{{\phi_b^*}^2} + \left(\frac{\tau_R^+}{\phi_{vD}^*}\right)^2 = \left(\frac{\tau^+}{\phi_t^*}\right)^2. \tag{12}$$

When compared to the formulation in the GFM transformation, Eq. (12) shares ϕ_{TL}^* as the scaling in the viscous sublayer, allows scaling the buffer layer explicitly through ϕ_b^*, and specifies the log layer scaling to be ϕ_{vD}^* (Eq. 9). The total, stress-based scaling, ϕ_t^*, can then be solved for:

$$\phi_t^* = \frac{\phi_b^*\phi_{vD}^*}{\sqrt{\left(\phi_b^*\phi_{vD}^*\right)^2 + 2\phi_{TL}^*(1-\phi_{TL}^*)(\phi_{vD}^*)^2 + \left((1-\phi_{TL}^*)\phi_b^*\right)^2}}, \tag{13}$$

where $\tau_v^+ = \phi_{TL}^*$ from the TL transformation, $\tau_R^+ = \tau^+ - \tau_v^+$ from the stress balance (Eq. 10), and τ^+ is taken to be unity. The last assumption is for convenience, since the complete stress profile is normally not available *a priori*, and it minimally impacts the scaling [15, 29]. Replacing ϕ_{vD}^* with the quasi-equilibrium assumption ($\phi_{vD}^* \rightarrow S_{eq}^+$) and setting ${\phi_b^*}^2 = S_{TL}^+ S_{eq}^+$ in Eq. (13) gives back the GFM transformation (Eq. 8).

1. Buffer Layer Scaling

The present transformation remains incomplete without a definition for the scaling in the buffer layer, ϕ_b^*. Classically, the buffer layer treatment adopted an asymptotic analysis approach, where the viscous and log regions were extrapolated beyond their range of validity to provide a matching condition. In the context of the three most successful mean velocity transformations to date (the vD, TL, and GFM), this is no different: van Driest [3] relies purely on log layer arguments, Trettel and Larsson [9] focus on the viscous sublayer, while Griffin *et al.* [15] interpolate between the two through a stress balance. With the exception of Wu *et al.* [12], who proposed a separate scaling for each sub-region of the boundary layer (including the buffer layer) based on Prandtl's mixing length, there were no attempts to collapse the buffer region. Even in the Wu *et al.* transformation, the bounds of each sublayer, and consequently the mapping function, had to be manually tuned depending on the wall-to-recovery temperature ratio, T_r/T_w [12]. While they attempted to generalize the limits, their transformation suffered from a lack of universality, as evident by the results of Volpiani *et al* [13]. This drawback is alleviated herein, since the relative magnitudes of τ_v^+ and τ_R^+ and their product, $\tau_v^+\tau_R^+$, automatically dictates the inner layer scaling and applies the appropriate normalization.

From the TKE budget, a few observations can be made regarding the buffer layer. First, the semi-locally normalized production term, P^*, is invariant when plotted against y^* for $y^* \lesssim 10$. Second, the maximum of P^* consistently falls within the buffer region, with a peak around $y^* \approx 11$ [11, 29]. Third, viscous dissipation, ϕ^* or ϕ^+, is much more significant than in the log region. Together with the fact that $P^* = \tau_v^+\tau_R^+$, these findings hint that the quasi-equilibrium assumption of Griffin *et al.* [15] is applicable there. In addition to the aforementioned observations, the latest numerical simulations of Huang *et al.* [27] and assessment of Bai *et al.* [32] corroborate the fact that the TL transformation is well-suited to scale the onset of the buffer region. Motivated by this, we scale the buffer layer with:

$$\phi_b^* = \phi_{TL}^* \frac{S_{eq}^+}{\phi_{vD}^*} = \frac{1}{\sqrt{\bar{\rho}^+}} \frac{dy^*}{dy^+} \frac{du^+}{dy^*}, \tag{14}$$

where ϕ_{TL}^* accounts for the viscous contribution to the buffer layer, emanating from the viscous sublayer, and S_{eq}^+/ϕ_{vD}^* scales the Reynolds stress, which first emerges in the buffer layer and asymptotes to τ_w in the log region. From a physical standpoint, S_{eq}^+/ϕ_{vD}^* resembles a weighting that combines the effects of quasi-equilibrium and vorticity transport in the dynamics of near-wall turbulence. Note that on the basis of temperature alone, $\phi_{TL}^* \propto \bar{T}^{+^{0.7}}$ since $\bar{\mu}^+ \sim \bar{T}^{+^{0.7}}$ [33] and $\phi_{vD}^* \propto \bar{T}^{+^{-1/2}}$ as a result of $\sqrt{\bar{\rho}^+} \sim \bar{T}^{+^{-1/2}}$. Thus, $\phi_b^* \propto \bar{T}^{+^{1/2}}$ lies within the bounds governing the viscous and log sub-regions and can be viewed to provide a smooth transition between the two.

III. Results

The final form of the proposed transformation is given by Eq. (13), where $\phi_{TL}^* = du_{TL}^+/dy^*$, $\phi_{vD}^* = du_{vD}^+/dy^*$ (Eq. 9), and $\phi_b^* = \phi_{TL}^* S_{eq}^+/\phi_{vD}^*$ (Eq. 14). Performing the integral in Eq. (4) with $\phi^\dagger = \phi_t^*$ and $y^\dagger = y^*$ then retrieves the non-dimensionalized mean velocity in the near-wall region, $u^+(y^*)$. The transformation is tested in two steps. One, the validity of ϕ_{vD}^* and ϕ_b^* is assessed. Two, its overall performance in the entire inner layer is evaluated. To ensure a consistent and broad comparison, supersonic pipe [25] and adiabatic and non-adiabatic high-speed channel [9, 14, 28] and boundary layer [11, 23, 24] flows at $Re_\tau^* > 200$ will be studied; this comprises a similar dataset to the one considered in Griffin *et al* [15]. For completeness, an evaluation will also be conducted on the supercritical boundary layer dataset of Kawai [34] and the supercritical channel data of Wan *et al.* [35], where the GFM transformation fell short in collapsing the profiles [32]. In all the cases, the scaling variables and velocity profiles will be compared against the incompressible channel results of Lee and Moser [36] obtained at $Re_\tau = 5200$.

A. Validity of ϕ_{vD}^* and ϕ_b^*

Figure 1 plots the diagnostic functions, $\phi_t^* y^*$ from the present paper, $S_t^+ y^*$ from the GFM transformation [15], $\phi_{VI}^* y^*$ from the Volpiani *et al.* data-driven transformation [13], and $\phi_{TL}^* y^*$ from the TL transformation [9], against the incompressible reference for both internal and external flows. As Patel *et al.* [10] assert, invariance of these quantities to the global flow parameters is critical to getting a collapse with the law of the wall. In addition, the sum of the error in

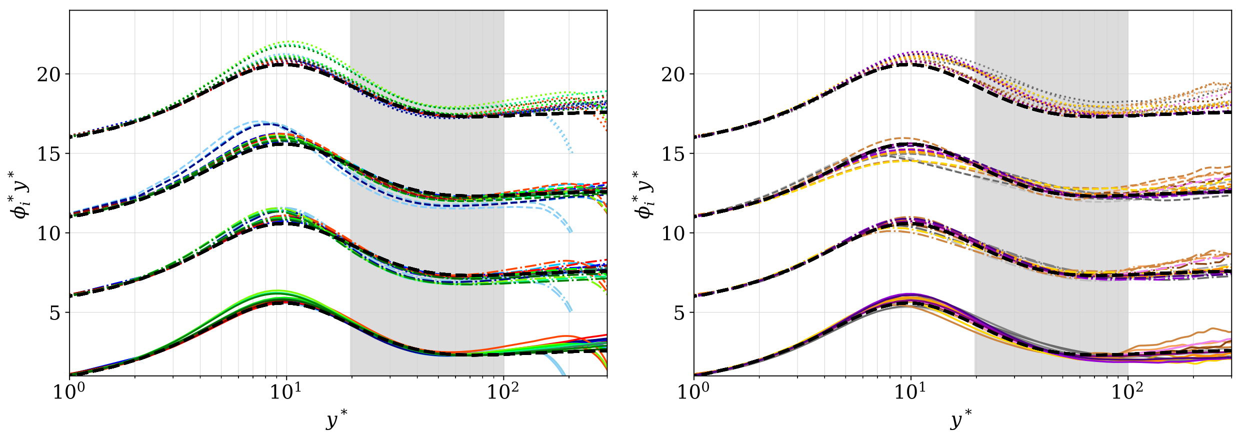

(a) Pipe and channel flows **(b) Boundary layer flows**

Fig. 1 Pre-multiplied, non-dimensionalized mean shear compared to the incompressible reference [36] (dashed black line). Colored lines are: blue [9], red [14, 25], green [28], gray [11], orange [23, 24], and purple [29]. Solid lines show $\phi_t^* y^*$ from the present scaling, while the dashed-dotted, dashed, and dotted lines show $S_t^+ y^*$, $\phi_{VI}^* y^*$, and $\phi_{TL}^* y^*$ from the GFM [15], Volpiani *et al.* [13], and TL [9] transformations, respectively, each offset by 5 units for clarity.

the log region from both functions is computed (Figure 2):

$$\Delta = \frac{\int_{y_1^*}^{y_2^*} \left| \phi_i^* y^* - \frac{du^+}{dy^+} y^+ \right| dy^*}{\int_{y_1^*}^{y_2^*} \left(\frac{du^+}{dy^+} y^+ \right) dy^*}, \tag{15}$$

where $\phi_i^* = \phi_t^*, S_t^+, \phi_{VI}^*,$ or ϕ_{TL}^*, $y_1^* = 20$, and $y_2^* = 100$. As can be seen, for internal flows, the error from the proposed scaling is consistently smaller than the quasi-equilibrium assumption of Griffin *et al* [15]. This finding was previously alluded to by Modesti and Pirozzoli [14], who theorized that the vD transformation will recover its accuracy as the bulk Reynolds number is increased, $Re_b \to \infty$, in compressible channel flows. Here, we show that the gradient of the integrated vD velocity profiles becomes extremely accurate in collapsing the log region when scaled by the semi-local wall-normal coordinate (the lines from ϕ_t^* are almost perfectly collapsed for $y^* > 20$). For boundary layer flows, the results demonstrate similar degrees of success as the GFM transformation, with $\phi_t^* y^*$ outperforming $S_t^+ y^*$ in some instances—this is evident by the fact that the error incurred from both variables is comparable, being lower than that obtained by the TL transformation (Figure 2). As such, relying on the semi-local mean spanwise vorticity, as given by ϕ_{vD}^*, as a basis for the scaling outside the viscous and buffer sublayers is reasonable.

B. Performance in the Inner Layer

The normalized velocity profiles from the vD, TL, GFM, and present transformations are shown in Figures 3 and 4 for pipe and channel and boundary layer flows, respectively. Figure 3 shows that the present transformation succeeds in

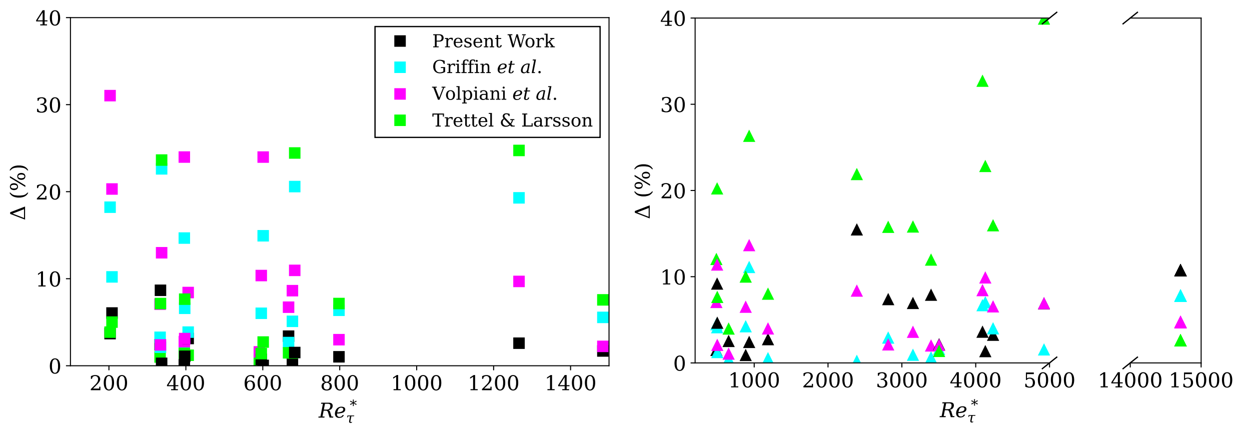

(a) Pipe and channel flows

(b) Boundary layer flows

Fig. 2 Total error in the log region, computed using Eq. (15)**, as a function of the semi-local friction Reynolds number for the dataset presented in Figure 1. Squares denote pipe and channel flows, whereas triangles correspond to boundary layer flows; colors differentiate each transformation.**

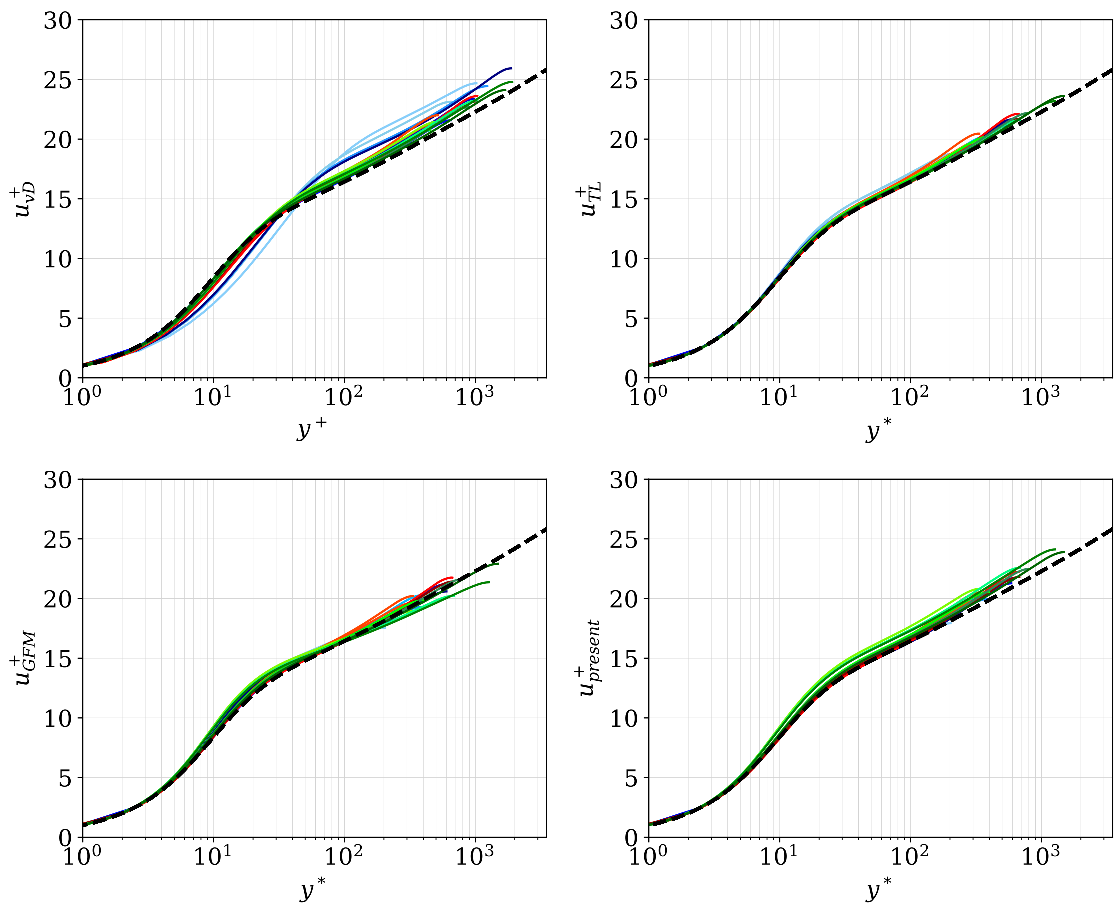

Fig. 3 Normalized mean-velocity profiles using the van Driest [3], Trettel and Larsson [9], Griffin *et al.* [15], and present transformation. Results shown are for internal flows, with and without wall cooling. See caption of Figure 1 for more details on the dataset and a description of the colors.

capturing the correct slope in the log layer, unlike the GFM transformation where Re_τ^* effects seem to deteriorate the collapse in the log region (green lines slope downward and diverge from the incompressible reference). Moreover, for internal flows, the collapse from the TL transformation remains far superior than any of the other transformations; this is expected since the scaled viscous stress was found to be invariant to the freestream and boundary conditions in the whole inner layer by Patel *et al* [10]. For external flows, however, the present transformation performs significantly better than the vD and TL transformations, and the performance is visually indistinguishable from, and very similar to, the GFM transformation. Looking back at Figures 1 and 2, one can note that the success of the GFM transformation is not due to the profile of $S_t^+ y^*$ exactly tracing the incompressible reference (dashed line in Figure 1). But, the success is in fact due to $S_t^+ y^*$ overshooting the incompressible reference in the buffer layer by the exact same amount it undershoots it with in the log layer. Thus, error cancellation takes place and the scaled velocity profiles collapse. This is also more clearly highlighted by Figure 3, where the profiles from the GFM transformation demonstrate less spread than the present transformation despite having larger overall integrated percent error (Figure 2).

In Figure 5, the present transformation is tested against the heated and unheated turbulent boundary layer data of Kawai [34] and differentially heated channel of Wan *et al.* [35], both at supercritical pressures. These specific datasets pose an interesting challenge for the current transformation for two reasons: (1) the flow contains non-negligible, non-linear real-fluid effects and (2) Bai *et al.* [32] showed that the GFM transformation is not able to capture the slope or recover the incompressible profile in the log layer of the scaled velocity. As can be seen, for boundary layer data, the present transformation yields an accurate collapse with the incompressible reference. In particular, the slope of the log layer is well captured, and the scaled profiles generally deviate only slightly from the reference curve. For channel flows, though, the vD and TL transformations remain wholly more accurate than the GFM and present transformations. While it could be deduced that vorticity transport may be a more reliable mechanism than the quasi-equilibrium assumption at supercritical conditions, since when used as a basis for the scaling in the log layer ϕ_{vD}^* recovers the log layer slope but quasi-equilibrium does not, a more in-depth investigation encompassing a variety of other flows is necessary to firmly establish this hypothesis. This is left for future work.

IV. Conclusions

Von Kármán's law of the wall has been a cornerstone in studies of canonical wall-bounded turbulence. It simply offers a way of attaining universality in incompressible flows with zero pressure gradient. To this end, several extensions have been made on the original formulation, to scale more complicated flows and include boundary conditions not initially part of the derivation. In flows where compressibility effects are dominant, the van Driest transformation has particularly stood the test of time, as it was shown to remain valid at very large freestream Mach numbers. However, as computational and experimental efforts expanded into high-speed flows with external wall heat transfer, its failure became pronounced.

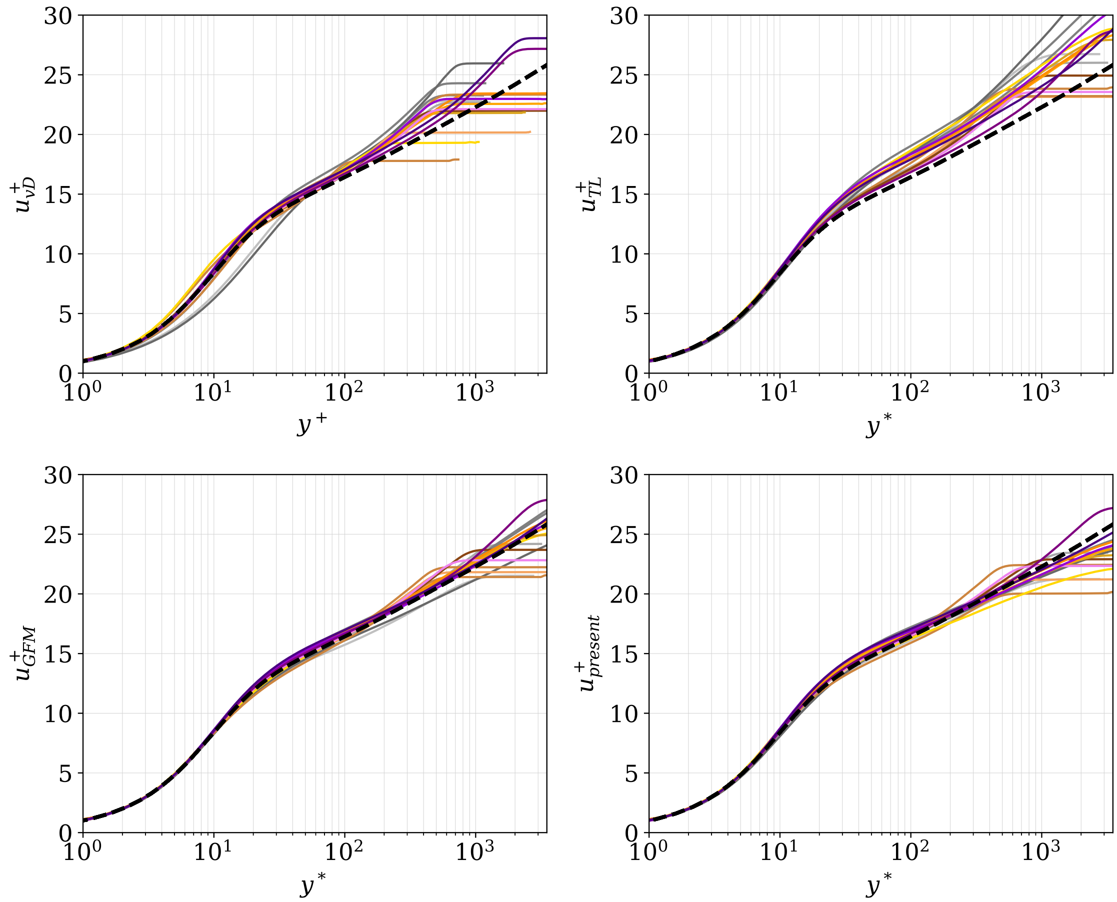

Fig. 4 Normalized mean-velocity profiles using the van Driest [3], Trettel and Larsson [9], Griffin *et al.* [15], and present transformation. Results shown are for boundary layer flows, with and without wall cooling. See caption of Figure 1 for more details on the dataset and a description of the colors.

Over the years, many efforts were undertaken to reconcile those failures. By far the most prominent approach has been that of Trettel and Larsson [9], who were successfully able to scale non-adiabatic, hypersonic channel flows back into the incompressible law of the wall. Yet, their transformation was not successful in the context of boundary layers. An extension was presented by Griffin *et al.* [15] using a total, stress-based approach and the assumption of quasi-equilibrium between turbulent kinetic energy production and dissipation in the log layer. Despite that, it remains unclear as to how and under what conditions does quasi-equilibrium hold. This paper revisits this assumption and presents a new transformation based on the semi-local van Driest velocity gradient, which is, in turn, rooted physically in the mechanism of vorticity transport in the boundary layer. The present approach also relies on a total stress balance, but it differs by explicitly allowing for a scaling in the buffer sublayer.

The performance of the new transformation is assessed by scaling the near-wall mean velocity profiles of published DNS simulations conducted at various Mach numbers and subject to wall cooling and heating. Both boundary layer and channel flows were considered, and the transformation produced excellent collapse irrespective of the boundary and

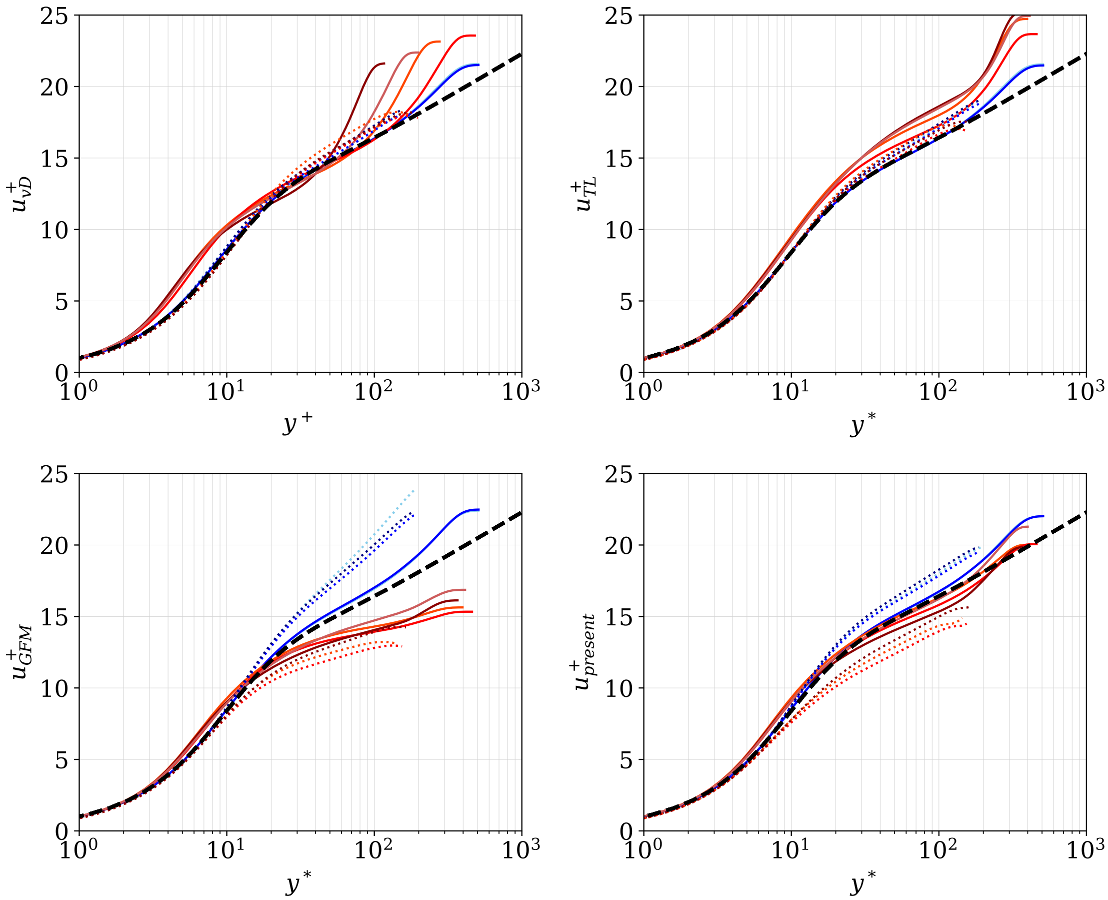

Fig. 5 Normalized mean-velocity profiles of the supercritical boundary layer data of Kawai [34] and channel data of Wan *et al.* [35] using the van Driest [3], Trettel and Larsson [9], Griffin *et al.* [15], and present transformation. Colors lines are: (blue) unheated/cold and (red) heated/hot. Solid lines correspond to boundary layer results [34]; dotted lines are channel data [35]. All cases plotted have $Re_\tau^* > 200$.

freestream conditions. Finally, the transformation was tested on turbulent boundary layer and channel data at supercritical pressure conditions. Whereas the Griffin *et al.* [15] transformation failed for boundary layers, the present transformation was found to give satisfactory collapse. For supercritical channel flows, neither the Griffin *et al.* [15] nor the current transformation yielded an improved collapse over the van Driest [3] and Trettel and Larsson [9] transformations. This offers an interesting avenue for future exploration.

Acknowledgments

K.Y. acknowledges financial support from the Natural Science and Engineering Research Council of Canada (NSERC). K.Y. is also indebted to Michele Cogo and Teng Wan for making their DNS data available.

References

[1] Kolmogorov, A. N., "Dissipation of energy in the locally isotropic turbulence," *Proceedings of the Royal Society of London. Series A: Mathematical and Physical Sciences*, Vol. 434, No. 1890, 1991, pp. 15–17. https://doi.org/10.1098/rspa.1991.0076, URL https://royalsocietypublishing.org/doi/10.1098/rspa.1991.0076.

[2] Karman, T. v., "Mechanical Similitude and Turbulence," Tech. rep., NACA Technical Memorandum 611, 1931.

[3] Van Driest, E. R., "Turbulent Boundary Layer in Compressible Fluids," *Journal of the Aeronautical Sciences*, Vol. 18, No. 3, 1951, pp. 145–160. https://doi.org/10.2514/8.1895.

[4] Danberg, J. E., "Characteristics of the turbulent boundary layer with heat and mass transfer at M = 6.7," Ph.D. thesis, Catholic University of America, 1964.

[5] Brun, C., Petrovan Boiarciuc, M., Haberkorn, M., and Comte, P., "Large eddy simulation of compressible channel flow: Arguments in favour of universality of compressible turbulent wall bounded flows," *Theoretical and Computational Fluid Dynamics*, Vol. 22, 2008, pp. 189–212. https://doi.org/10.1007/s00162-007-0073-y.

[6] Cope, W. F., and Hartree, D. R., "The laminar boundary layer in compressible flow," *Philosophical Transactions of the Royal Society of London. Series A, Mathematical and Physical Sciences*, Vol. 241, No. 827, 1948. https://doi.org/10.1098/rsta.1948.0008.

[7] Zhang, Y. S., Bi, W. T., Hussain, F., Li, X. L., and She, Z. S., "Mach-number-invariant mean-velocity profile of compressible turbulent boundary layers," *Physical Review Letters*, Vol. 109, No. 054502, 2012. https://doi.org/10.1103/PhysRevLett.109.054502.

[8] Pei, J., Chen, J., Fazle, H., and She, Z., "New scaling for compressible wall turbulence," *Science China: Physics, Mechanics and Astronomy*, Vol. 56, No. 9, 2013, pp. 1770–1781. https://doi.org/10.1007/s11433-013-5147-9.

[9] Trettel, A., and Larsson, J., "Mean velocity scaling for compressible wall turbulence with heat transfer," *Physics of Fluids*, Vol. 28, No. 026102, 2016. https://doi.org/10.1063/1.4942022.

[10] Patel, A., Boersma, B. J., and Pecnik, R., "The influence of near-wall density and viscosity gradients on turbulence in channel flows," *Journal of Fluid Mechanics*, Vol. 809, 2016, pp. 793–820. https://doi.org/10.1017/jfm.2016.689.

[11] Zhang, C., Duan, L., and Choudhari, M. M., "Direct numerical simulation database for supersonic and hypersonic turbulent boundary layers," *AIAA Journal*, Vol. 56, No. 11, 2018, pp. 4297–4311. https://doi.org/10.2514/1.J057296.

[12] Wu, B., Bi, W., Hussain, F., and She, Z. S., "On the invariant mean velocity profile for compressible turbulent boundary layers," *Journal of Turbulence*, Vol. 18, No. 2, 2017, pp. 186–202. https://doi.org/10.1080/14685248.2016.1269911.

[13] Volpiani, P. S., Iyer, P. S., Pirozzoli, S., and Larsson, J., "Data-driven compressibility transformation for turbulent wall layers," *Physical Review Fluids*, Vol. 5, No. 5, 2020, p. 052602. https://doi.org/10.1103/PhysRevFluids.5.052602.

[14] Modesti, D., and Pirozzoli, S., “Reynolds and Mach number effects in compressible turbulent channel flow,” *International Journal of Heat and Fluid Flow*, Vol. 59, 2016, pp. 33–49. https://doi.org/10.1016/j.ijheatfluidflow.2016.01.007.

[15] Griffin, K. P., Fu, L., and Moin, P., “Velocity transformation for compressible wall-bounded turbulent flows with and without heat transfer,” *Proceedings of the National Academy of Sciences*, Vol. 118, No. 34, 2021, p. e2111144118. https://doi.org/10.1073/pnas.2111144118.

[16] Duan, L., Beekman, I., and Martín, M. P., “Direct numerical simulation of hypersonic turbulent boundary layers. Part 3. Effect of Mach number,” *Journal of Fluid Mechanics*, Vol. 672, 2011, pp. 245–267. https://doi.org/10.1017/S0022112010005902.

[17] Duan, L., Beekman, I., and Martín, M. P., “Direct numerical simulation of hypersonic turbulent boundary layers. Part 2. Effect of wall temperature,” *Journal of Fluid Mechanics*, Vol. 655, 2010, pp. 419–445. https://doi.org/10.1017/S0022112010000959.

[18] Pirozzoli, S., and Bernardini, M., “Turbulence in supersonic boundary layers at moderate Reynolds number,” *Journal of Fluid Mechanics*, Vol. 688, 2011, pp. 120–168. https://doi.org/10.1017/jfm.2011.368.

[19] Eyink, G. L., “Turbulent flow in pipes and channels as cross-stream “inverse cascades” of vorticity,” *Physics of Fluids*, Vol. 20, No. 12, 2008, p. 125101. https://doi.org/10.1063/1.3013635.

[20] Morkovin, M. V., “Effects of compressibility on turbulent flows,” *Mécanique de la Turbulence*, 1962, pp. 367–380.

[21] Trettel, A. J., *Velocity transformation for compressible wall turbulence with heat transfer*, University of Maryland, MSc Thesis, 2015.

[22] Younes, K., *Velocity scaling of high-speed turbulent boundary layer flows with wall heat transfer*, University of Waterloo, MSc Thesis, 2021. URL http://hdl.handle.net/10012/17147.

[23] Volpiani, P. S., Bernardini, M., and Larsson, J., “Effects of a nonadiabatic wall on supersonic shock/boundary-layer interactions,” *Physical Review Fluids*, Vol. 3, No. 8, 2018. https://doi.org/10.1103/PhysRevFluids.3.083401.

[24] Volpiani, P. S., Bernardini, M., and Larsson, J., “Effects of a nonadiabatic wall on hypersonic shock/boundary-layer interactions,” *Phys. Rev. Fluids*, Vol. 5, No. 014602, 2020. https://doi.org/10.1103/PhysRevFluids.5.014602.

[25] Modesti, D., and Pirozzoli, S., “Direct numerical simulation of supersonic pipe flow at moderate Reynolds number,” *International Journal of Heat and Fluid Flow*, Vol. 76, 2019, pp. 100–112. https://doi.org/10.1016/j.ijheatfluidflow.2019.02.001.

[26] Huang, J., Nicholson, G. L., Duan, L., Choudhari, M. M., and Bowersox, R. D., “Simulation and Modeling of Cold-Wall Hypersonic Turbulent Boundary Layers on Flat Plate,” *AIAA Scitech 2020 Forum*, American Institute of Aeronautics and Astronautics, Reston, Virginia, 2020. https://doi.org/10.2514/6.2020-0571.

[27] Huang, J., Duan, L., and Choudhari, M. M., “Direct numerical simulation of hypersonic turbulent boundary layers: effect of spatial evolution and Reynolds number,” *Journal of Fluid Mechanics*, Vol. 937, 2022. https://doi.org/10.1017/jfm.2022.80.

[28] Yao, J., and Hussain, F., "Turbulence statistics and coherent structures in compressible channel flow," *Physical Review Fluids*, Vol. 5, No. 8, 2020. https://doi.org/10.1103/PhysRevFluids.5.084603.

[29] Cogo, M., Salvadore, F., Picano, F., and Bernardini, M., "Direct numerical simulation of supersonic and hypersonic turbulent boundary layers at moderate-high Reynolds numbers and isothermal wall condition," *Journal of Fluid Mechanics*, Vol. 945, 2022, p. A30. https://doi.org/10.1017/jfm.2022.574, URL https://www.cambridge.org/core/product/identifier/S0022112022005742/type/journal_article.

[30] Huang, P. G., Coleman, G. N., and Bradshaw, P., "Compressible turbulent channel flows: DNS results and modelling," *Journal of Fluid Mechanics*, Vol. 305, 1995, pp. 185–218. https://doi.org/10.1017/S0022112095004599.

[31] Fernholz, H. H., and Finley, P. J., "A Critical Commentary on Mean Flow Data for Two-Dimensional Compressible Turbulent Boundary Layers," Tech. rep., NATO AGARD-AG-253, 1980.

[32] Bai, T., Griffin, K. P., and Fu, L., "Compressible Velocity Transformations for Various Noncanonical Wall-Bounded Turbulent Flows," *AIAA Journal*, Vol. 60, No. 7, 2022, pp. 4325–4337. https://doi.org/10.2514/1.J061554.

[33] Smits, A. J., and Dussauge, J.-P., *Turbulent Shear Layers in Supersonic Flow*, Springer, New York, 2006.

[34] Kawai, S., "Heated transcritical and unheated non-transcritical turbulent boundary layers at supercritical pressures," *Journal of Fluid Mechanics*, Vol. 865, 2019, pp. 563–601. https://doi.org/10.1017/jfm.2019.13.

[35] Wan, T., Zhao, P., Liu, J., Wang, C., and Lei, M., "Mean velocity and temperature scaling for near-wall turbulence with heat transfer at supercritical pressure," *Physics of Fluids*, Vol. 32, No. 5, 2020. https://doi.org/10.1063/5.0002855.

[36] Lee, M., and Moser, R. D., "Direct numerical simulation of turbulent channel flow up to Re$_\tau$ $\approx$ 5200," *Journal of Fluid Mechanics*, Vol. 774, 2015, pp. 395–415. https://doi.org/10.1017/jfm.2015.268.